MODELLING OF A WARPING WING FOR ENERGY CONSUMPTION MINIMIZATION

M. Bolinches i Gisbert , A. J. Keane , A. J. Forrester
University of Southampton
m.bolinches_i_gisbert@soton.ac.uk; Andy.Keane@soton.ac.uk;
Alexander.Forrester@soton.ac.uk

Keywords: *morphing wing, warping, buckling, energy reduction*

Abstract

Morphing structures and, in particular, morphing wings require of large amounts of energy. This energy is used up in two different processes. Some of this energy is used as 'useful' energy and fights the external loads (aerodynamic pressure in the case considered here). The rest of the energy is used to make the previous process possible. In this case this energy is used in deforming the material (in the case of a hinged mechanical actuator this energy would be used to fight friction and inertial forces, for instance). If the material being deformed is part of a structural component this energy will be high, in fact considerable higher than the actual energy needed to overcome the external loads ('useful' energy) and it is, therefore, necessary to design systems that can deform more with less deformation energy. In this paper, this problem is tackled by the usage of buckled structures. In essence, the lower surface of the wing is compressed with springs so large deformations are achieved with low actuating forces. This concept is compared against a similar warping wing without buckled skin demonstrating substantial energy savings.

1 Introduction

Changing the shape of a wing in order to manoeuvre an aircraft has been done since the beginnings of aviation. The Wright brothers' Flyer used warping of the wings to achieve roll control. In the successive years aircraft became heavier as more payload was wanted to get on-board and cruise-speed increased. With heavier aircraft the wings were made stiffer in order to withstand higher loads and hence warping was difficult to achieve. This led to the use of ailerons. These systems decouple the load-carrying structure and the deformation which occur around a hinge bringing the actuating forces down. Although this is advantageous as it decouples both effects this led to other difficulties. Aileron reversal appears as the camber discontinuity increases sharply the pitching moment. Also, separation may occur at this hinge location which decreases performance in manoeuvres (e.g., turns).

Several studies suggest that the use of morphing structures or morphing vehicles can provide advantageous performance over conventional configurations [1, 2]. For instance, in the work by Khot et al. [1], it is explained that the use of twist of the wing to provide roll control has the advantage of not having reversal effect at hight dynamic pressure. Though a good improvement, it does come as a high cost in terms of energy consumption and required actuating forces.

Austing et al. [3] show another application of a morphing concept. In their work they reduce the shock-induced drag of an aerofoil. This is a very beneficial application as aerofoils designed to operate in the subsonic design can then be used at higher speeds enhancing the aircraft flight envelope. Although the concept was tested experimentally this still requires of some improvements

especially in the actuator front as it requires high and heavy actuators.

Not only these systems can provide an advantage over conventional systems in terms of manoeuvrability and drag reductions but also they can improve the flight envelope by flutter suppression. For instance in the work by McGowan [4] several methods for load alleviation and flutter suppression are considered which show the increasing interest in these technologies.

The problem with all these systems is the amount of energy required to perform the changes on the structure that provide the performance benefit. This is acknowledged by many of the authors and is indeed source of active research [6, 5, 7]. Namgoong et al. [6], for instance, recommend the addition of energy considerations during aerodynamic optimisation and propose a method to account for the strain energy required (based on linear springs) to morph between a given aerofoil shape and any other shape optimised for a different aerodynamic condition. In they work several studies are carried out that highlight the different geometries achieved when including energy considerations in the optimisation against the purely aerodynamic method. In the work by Gern et al [5] they study the application of an array of distributed actuators over a wing and compare it against the same wing with ailerons. It is shown how at low dynamic pressures the energy required to provide the same roll performance as a conventional wing is much higher for the morphing one. The situation is the opposite when the dynamic pressure has gone beyond the conventional wing reversal dynamic pressure.

Due to the large amount of energy required to produce acceptable levels of roll a part of the research of morphing and compliant mechanisms has been focused on reducing this energy. A clever approach has been the use of buckled structures. These structures require less input energy to be deformed. This is the case studied by Vos et al. [8]. In their work they study the usage of actuators with embedded piezoelectric actuators which they pre-compress and which they call pre-compressed piezoelectric actuators (PBP). In the case studied by Vos et al. the actuator was compressed by the skin and they managed to achieve a roll authority 38% higher than with the use of ailerons and a weight saving of 3.5%.

The work presented here shows our results on reducing the energy requirement for a warping wing design for a small unmanned aerial vehicle (UAV) making use of buckled structures in which spring energy is used to provoke the buckling. An initial wing concept was designed and tested both in-flight and in the wind-tunnel which worked as a proof-of-concept. It was realised that high current was drawn from the servos indicating the need for study in the lines of reducing energy requirements. The initial concept as well as the new modified concept are described in section 2. A description of the numerical model can be read in section 3. The rest of this work is devoted to the exploitation of the system. Computations are made to understand what is the behaviour of the wing with varying spring properties and an assessment of the energy saving is made.

2 Wing concept

The design of a wing for warping is a complicated task. On the one hand it has to be flexible enough as for the actuating loads deforming the structure to be low enough so the system is viable. On the other hand the structure has to have the rigidity to withstand the aerodynamic loads. These are contradicting requirements which need to be tackled simultaneously.

The wing concept (this concept was analysed in [10]) presented here is based on open cross-section beams. It is known from beam theory (see, for instance, [9]) that open cross-sections beams present much lower torsion rigidity than the closed counterparts as seen from equations 1 and 2

$$J_{\text{closed}} = \frac{4A^2}{\oint \frac{ds}{t}} \tag{1}$$

$$J_{\text{open}} = \frac{1}{3}\int_{sect} t^3 ds \tag{2}$$

where A is the area enclosed by the beam cross-section, s is the a coordinate along the cross-

section line and t is the cross-section material thickness. J_{closed} and J_{open} are the torsional rigidity of the closed and open cross-sections respectively.

Figure 1 shows the way the open cross-section skin works. It can be seen that the section is opened at the profile trailing edge. Forces are applied at the two sides of this opening resulting in a change of camber of the airfoil. In order for the profile to deformed as shown (figure 1(b)) both sides of the opening are restrained to only slide over each other. This is, the sides of the opening are only allowed to move in the opening plane.

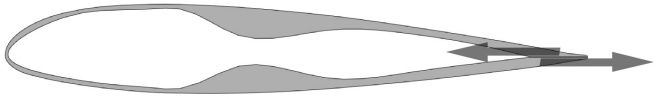

(a) Cross-section initial configuration and actuating loads.

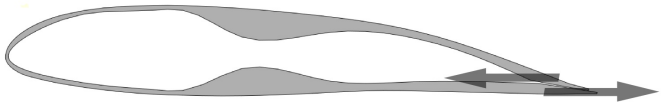

(b) Deformed cross-section.

Fig. 1 Schematic of how the open cross-section works.

The use of this concept resulted in large amounts of energy being used to drive the servos providing the actuating loads and alternative ways to reduce the load were sought. An alternative solution was studied that made use of structures in the post-buckled region. Structures in the post-buckled region (see the work by Narcis et al. [11]) present lower stiffness than in the linear regime hence providing a potential advantage when morphing. The idea is to buckle the lower surface skin in such a way that it provides the appropriate curvature. This curvature can then be changed with the actuating loads hence providing roll control. The idea would be as depicted in figure 2. As it can be seen in the figure the application of a force at the lower surface trailing edge provides large amount of displacement provided the surface buckles as seen. The problem is, therefore, to provide the force that buckles the surface before any loads are applied. This is, the actuator must only provide the force required to control the deformation but not the force required to buckle the surface. The way that is done in this work is by means of springs. Springs would be attached to the main spar of the structure (or any other fixed part) and linked to the lower surface (an array of these would be used). A schematic drawing of the concept can be seen in figure 3. The springs have reference lengths

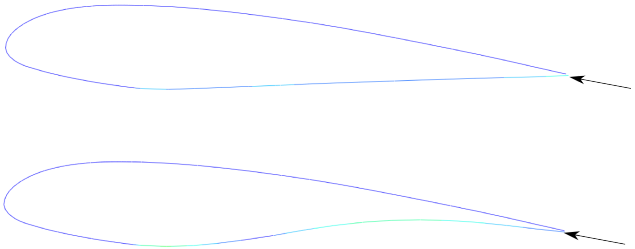

Fig. 2 Schematic of the buckled lower surface.

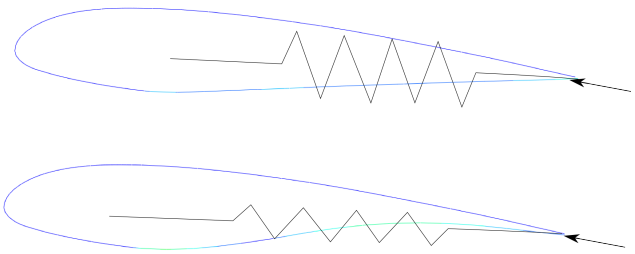

Fig. 3 Schematic of the buckled cross-section with spring.

shorter than the distance between the attachment point and the trailing edge point at its span-wise location, hence pulling the surface. These compression loads provide the buckling force.

3 Wing model

A numerical model of the concept previously explained was built. This model is flexible in order to allow for optimisation algorithms to operate over it. The main part of the model is structural as the problem is of an elastic nature. Nevertheless, aerodynamic coupling must be provided

as the flexibility of these structures can compromise the performance. Also, performance can be over-predicted if aeroelastic considerations are not taken into account.

3.1 Structural Model

The structural model is the main part of the simulation. This model generates the geometry according to the specified parameters, i.e., taper ratio, chord at root, aspect ratio, number of springs across the span direction to be modelled, etc. Some of the parameters are purely geometrical, that is, the shape of the modelled wing. Additionally, there are a set of parameters that influence the buckling behaviour. These are related, in turn, to the spring characteristics. Variables of this type include the spring stiffness coefficient (spring constant) and the reference length of individual springs. In order to reduce the number of variables two reduction rates of the reference length are defined: chord-wise reduction rate coefficient and span-wise reduction rate coefficient. The first one is related to length of the spring in relation to the local chord length, that is, how much shorter the spring is in relation to the chord; the latter, is an addition reduction of reference length depending on the spring span-wise position. This latter parameter changes the behaviour of the wing and the overall performance as it makes it more responsive to loading in different span-wise locations.

Examples of different achievable geometries can be seen in the following figure 4 where the dashed lines represent the springs. Extra cross-sections are defined to the sides of the actuating points (not represented in the figures). This is done in order to capture more details when transferring data to the aerodynamic code (section 3.2) in regions where higher deformations exist.

As well as the geometry the code written to generate the geometry also meshes the surfaces. Shell elements are used to model the skin and axial constraints are used to model the springs.

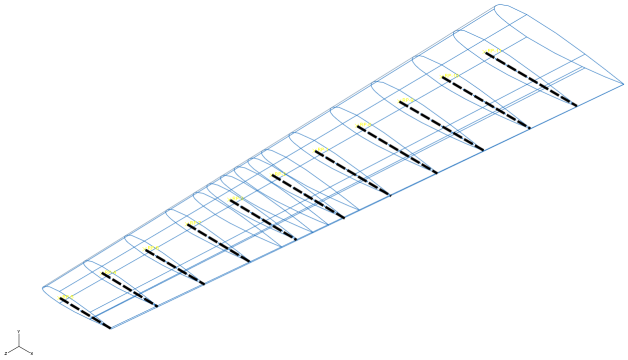

(a) Wing with 11 springs and taper ratio of 0.45.

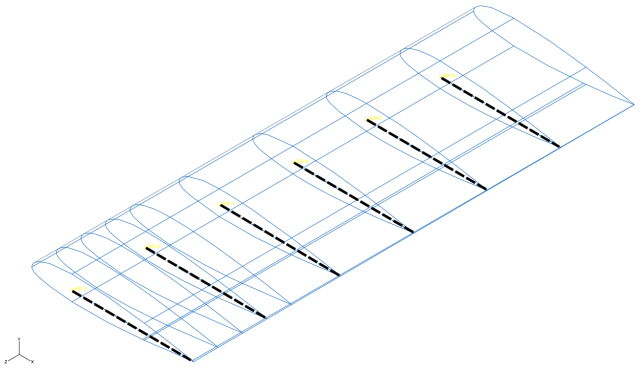

(b) Wing with 6 springs and no taper ratio.

Fig. 4 Examples of the generated geometries.

3.2 Aerodynamic Model

Aerodynamic analysis are carried out in order to compute the pressure distribution over the aerodynamic surfaces as well as to assess the performance of the system. These analyses are performed using a full potential equations solver [12]. This full potential method [12] (called FP) is coded in Fortran and computes the solution of the stationary inviscid equations (stationary Euler equations) of fluids by a method of finite differences. The necessary mesh for finite difference is also generated by these code using conformal transformations from the physical space to the computational space which consist of a cylinder of radius 1 and length 1. The Kutta-Joukovsky condition is satisfied at the trailing edge which require a vorticity sheet to be introduced emanating from the wing's trailing edge. This sheet is supposed to remain planar during the analysis and so roll-up effects are neglected. This is a rather good approximation at low angles

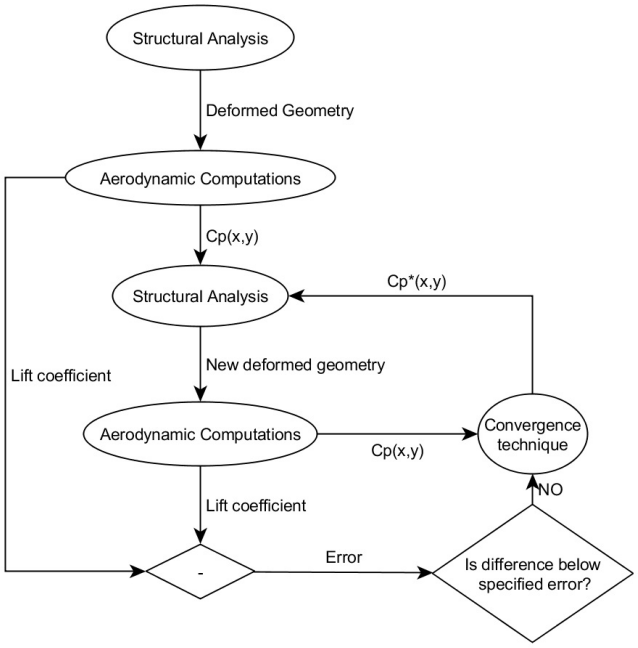

Fig. 5 Aerodynamics-Structure staggered coupling flowchart.

of attack.

3.3 Static Aeroelastic Coupling

Because the structure under consideration is of a flexible nature aeroelastic consideration must be taken into account. Without these considerations the performance of the wing could be over-predicted leading to false conclusions.

The approach followed here is a staggered approach. This is graphically described in figure 5 and goes as follows: Deformation due to actuation loads is computed without the effect of the aerodynamic loads. The aerodynamics characteristics of this deformed shape are then calculated. The resulting pressure distributions over the upper and lower surfaces are transferred to the structural model which is again run with these pressure loads. This process is then repeated until convergence of lift coefficient is achieved. In order to avoid "over-shooting" the pressure distributions are relaxed between structural analyses. That is, the pressure distribution of the last aerodynamic computation is linearly combined with the previous one as in equation 3 in order to stabilise the process (see also [13]).

$$\bar{C_P}^{n+1}(x,y) = k \cdot C_P^{n+1}(x,y) + (1-k) \cdot C_P^n(x,y) \tag{3}$$

In equation 3 x and y are the coordinates along the longitudinal axis of the aeroplane and the spanwise direction respectively.$C_P^n(x,y)$ is the pressure coefficient function at iteration n, $C_P^{n+1}(x,y)$ is the pressure distribution function at iteration $n+1$ and ${C_P}^{n+1}(x,y)$ is the pressure distribution function that is used for the following iteration $(n+2)$ provided convergence has not been achieved.

4 Computations

The main purpose of the lower surface to work in a post-buckled regime is purely to reduce the forces applied to actuate the wing. The amount of energy actually saved by reducing the actuating force is dependant on the actuating mechanism. In the case studied here electric servo-actuators are considered. For these actuators, the input electrical power is proportional to the output torque and hence the force. The proportionality between the force and the current draw[1] is roughly linear. Since the input power can be expressed as in equation 4

$$P(t) = V \cdot I(t) \tag{4}$$

where the voltage V is constant and the current draw I is a function of time, t; and the current draw can be considered linear with the output force as in equation 5

$$I(t) = k_{fe} \cdot F_{\text{actuating}} \tag{5}$$

where the constant k_{fe} is a proportionality constant that relates output force with electric current draw and $F_{\text{actuating}}$ is the actual output or actuating force; the input power can then be expressed as in equation 6.

$$P(t) = V \cdot k_{fe} \cdot F_{\text{actuating}} \tag{6}$$

[1] These servos function at constant voltage.

As seen in the equation (6) the power behaves linearly with the actuating force so when integrating the power over the same period of time, a decrease in the actuating force in half reduces the input power in the same amount.

One would, of course, be interested in increasing the slope of the curve $C_L(F_{\text{actuating}})$, this is, $\frac{\partial C_L}{\partial F_{\text{actuating}}}$. A study was performed to analyse what is the effect of the spring characteristics on this slope. In a first instance, a study was performed to analyse the effect of the reference length on slope. To this aim, different analyses with constant spring constant but varying reference lengths was performed and can be seen in figure 6. In the figure the spring constant is in all cases 0.05N/m. This high rigidity makes the lift to change strongly with the reference length variations but not much with the applied force. Also, as the reference length shortens further (see Figure 6(e)) high deformation of the lower surface occur leading to stall effects. Stall effects cannot be computed by the aerodynamic code. Instead, it fails to solve converging to previous values (before deformation occurs) which explains the shape of the curves.

As it can be noticed, the slope of the curves remains roughly constant with varying reference lengths (except for the cases when stall occurs). This suggests the slope is dependent on the spring constant. A similar experiment was carried out and the results can be seen in Figure 7. Compared with the graphs in Figure 6 the slope of Figure 7 is twice higher. Notice that the spring reduction is larger in this case. This is due to the inability of the spring to provide forces high enough as to provide enough force for buckling. The slope now seems to not vary linearly as before. These non-linearities seem to arise from the aeroelastic interaction as a more stretched surface tends to deform more under the aerodynamic pressure than a more bent surface (a more buckled surface).

A linear reduction of the reference length span-wise and chord-wise of 30% seems to provide the highest slope.These values will be used for the rest of the analysis.

4.1 Wing concepts comparison

This concept (buckled wing concept) is compared against the previous concept (explained in section 2). For both wings the same level of performance is demanded in order to compare the amounts of energy required to achieve this. Since the previous concept was optimised to achieve high roll authority, difference in lift coefficient between a camber-up and a camber-down deformation (equivalent to an aileron down and up deflection) is compared which is proportional to roll moment given the centre of pressure does not change heavily (this also assumes unsymmetrical wing loading plays a second-order effect on the semi-wing loading).

The following results are found. In order to achieve a difference in lift coefficient of 0.15 a force applied to the upper and lower surface of the previous concept of 10N for the “down” configuration and -10N for the “up” configuration is required, totalling 80N (two servos are used). For the buckled wing concept a 5N force for the up configuration applied to the lower surface only and -10N for the down configuration are required, totalling 30N. This means a reduction in applied force of over 60% which in turn, translates in the same energy reduction as explained above.

5 Conclusions

A new wing concept based in buckling of the lower surface has been explained as well as its numerical model. This concept uses an array of springs spread over the length of the wing to provoke the buckling of the lower surface. Once buckled, the wing is actuated at several locations. Both the number of springs and the actuation locations can be defined in the parametric model of the wing along with other geometric parameters.

It has been studied how the behaviour of the wing changes with the spring characteristics. In particular, the slope of the lift coefficient curve against actuating force has been analysed. This slope seems to not change in great measure with reference length provided stall effects do not occur. This slope does, however, changes with

spring stiffness.

The new wing concept has been compared against an previous concept optimised for roll control. Even with a non-optimised design this new concept is able to achieve the same performance level with over a 60% energy savings.

Future work should be aimed at further studying the materials employed as these affect the slope of the lift coefficient against actuation load curve. Optimisation should be run over the model to further exploit the capabilities of the model. After these, experimental validation should be done.

References

[1] N. S. Khot, K. Appa, J. Ausman and F. E. Eastep, *Deformation of a flexible wing using an actuating system for a roling maneuver without ailerons*. AIAA-98-1802, p.876-884, 1998.

[2] Daniel Coutu, Vladimir Brailovski and Patrick Terriault, *Promising Benefits of an Active-Extrados Morphing Laminar Wing*. *Engineering Notes, Journal of Aircraft*, vol. 46, No. 2, 2009, p. 730-731

[3] Fred Austin, Michael J. Rossi, William Van Nostrand, Gareth Knowles and Antony Jameson, *Static Shape Control for Adaptive Wings*. *AIAA Journa*,l vol.32. no.9, 1994, p.1895-1901.

[4] Anna-Maria R. McGowan, Lucas G. Horta, Joycelyn S. Harrison and David L. Raney, *Research activities within NASA's Morphing Program*. *RTO AVT Specialists' Meeting on Structural Aspects of Flexible Aircraft Control*, 1999, RTO MP-36, p. 13.1-13.10.

[5] Frack H. Gern, Daniel J. Inman and Rakesh K. Kapania, *Computation of Actuation Power Requirements for Smart Wings with Morphing Airfoils*. *AIAA Journal*, Vol. 43, No. 12, 2005, p. 2481-2486.

[6] Howoong Namgoong, William A. Crossley and Anastasios S. Lyrintzis, *Aerodynamic Optimization of a Morphing Airfoil Using Energy as an Objective*. *AIAA Journal*, Vol. 45, No. 9, 2007, p. 2113-2124.

[7] Christopher O. Johnston, William H. Manson. Cheolheui Han and Daniel J. Inman, *Actuator-Work Concepts Applied to Unconventional Aerodynamic Control Devices*. *Journal of Aircraft*, Vol. 44, No. 5, 2007, p. 1459-1468.

[8] Roelf Vos, Roeland De Breuker, Ron Barrett and Paolo Tiso, *Morphing Wing Flight Control Via Postbuckled Precompressed Piezoelectric Actuator*. *Journal of Aircraft*, vol. 44, No. 4, 2007, p. 1060-1068.

[9] Megson, T., *Aircraft Structures for Engineering Students*, Butterworth-Heinemann Ltd; 3rd Revised edition edition (30 April 1999)

[10] M. Bolinches, A. J. Keane, A. I. J. Forrester, J. P. Scanlan and K. Takeda, *Design, analysis and experimental validation of a morphing UAV wing*. The Aeronautical Journal, vol. 115, No. 1174, 2011, p.761-765

[11] Ursache, N.M., Bressloff, N.W. and Keane, A.J., *The design of post-buckled spinal structures for airfoil shape control using optimization methods*. *5th ASMO UK / ISSMO conference on Engineering Design Optimization* , 2004, p. 1-9

[12] ESDU, "Full-potential (FP) method for three-dimensional wings and wing-body combinations - inviscid flow Part 1: Principles and results", ESDU-02013, London, June 2002 with amendment A May 2006

[13] Huixue Dang, Zhichun Yang and Yi Li, *Accelerated loosely-coupled CFD/CSD method for nonlinear static aeroelasticity analysis*. Aerospace Science and Technology, vol. 14, No. 4, 2010, p. 250 - 258.

5.1 Copyright Statement

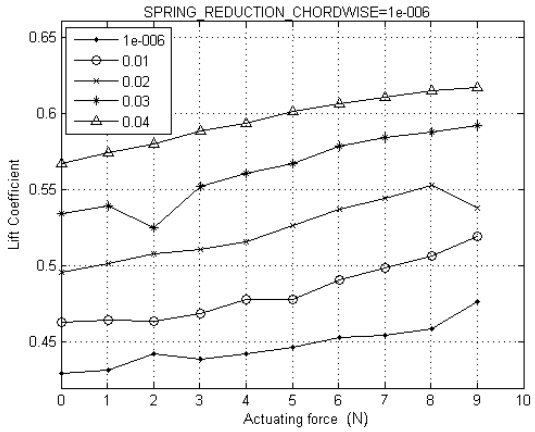

(a) Lift coefficient variation against actuating force for a chord-wise reference length reduction of 1E-6 and a reduction span-wise of 1E-6, 0.01, 0.03 and 0.04.

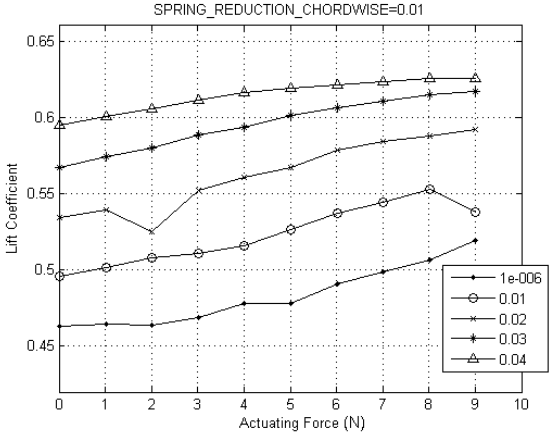

(b) Lift coefficient variation against actuating force for a chord-wise reference length reduction of 0.01 and a reduction span-wise of 1E-6, 0.01, 0.03 and 0.04.

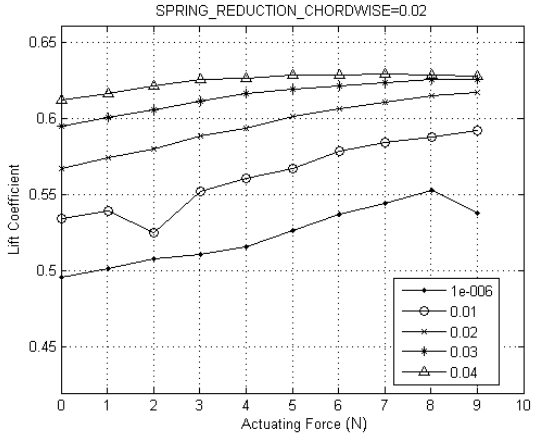

(c) Lift coefficient variation against actuating force for a chord-wise reference length reduction of 0.02 and a reduction span-wise of 1E-6, 0.01, 0.03 and 0.04.

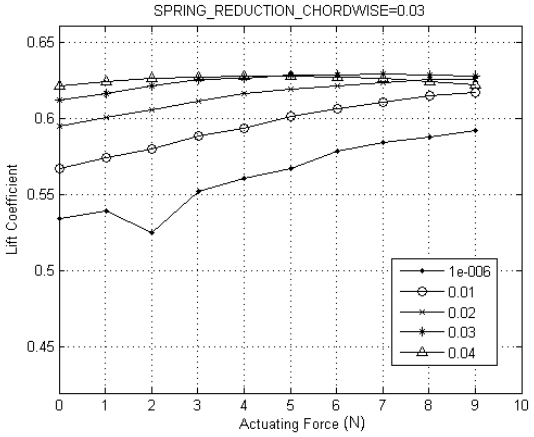

(d) Lift coefficient variation against actuating force for a chord-wise reference length reduction of 0.03 and a reduction span-wise of 1E-6, 0.01, 0.03 and 0.04.

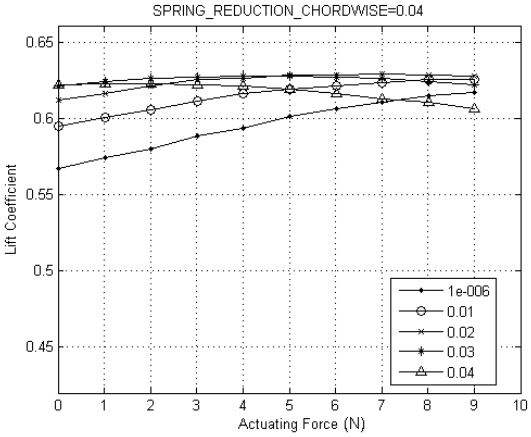

(e) Lift coefficient variation against actuating force for a chord-wise reference length reduction of 0.04 and a reduction span-wise of 1E-6, 0.01, 0.03 and 0.04.

Fig. 6 Variations of the curve $C_L(F_{\text{actuating}})$ with different values of the reference length defined by the percentage reductions chordwise and spanwise for a spring constant of 0.05N/m.

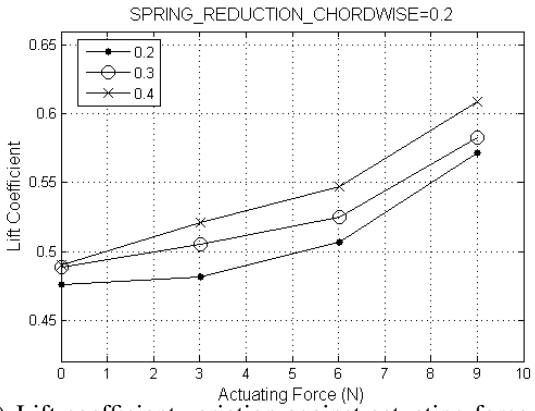

(a) Lift coefficient variation against actuating force for a chord-wise reference length reduction of 0.2 and a reduction span-wise of 0.2, 0.3 and 0.4.

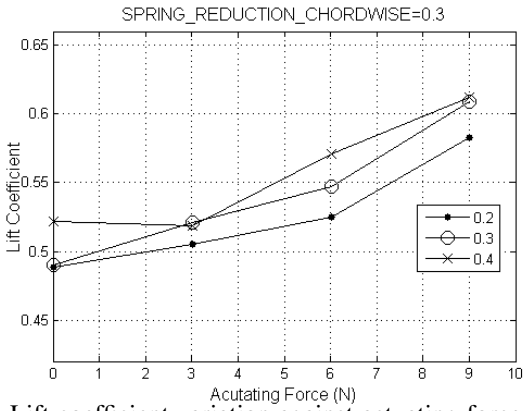

(b) Lift coefficient variation against actuating force for a chord-wise reference length reduction of 0.2 and a reduction span-wise of 0.2, 0.3 and 0.4.

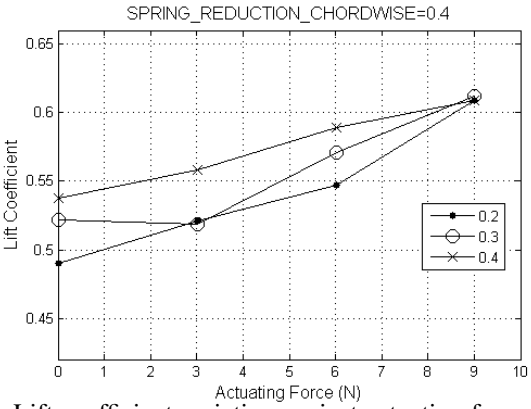

(c) Lift coefficient variation against actuating force for a chord-wise reference length reduction of 0.02 and a reduction span-wise of 0.2, 0.3 and 0.4.

Fig. 7 Variations of the curve $C_L(F_{\text{actuating}})$ with different values of the reference length defined by the percentage reductions chordwise and spanwise for a spring constant of 0.01N/m.